



Citation for published version:

Wilson, PB & Williams, IH 2018, 'Computational Modeling of a Caged Methyl Cation: Structure, Energetics, and Vibrational Analysis', *Journal of Physical Chemistry A*, vol. 122, no. 5, pp. 1432-1438.
<https://doi.org/10.1021/acs.jpca.7b11836>

DOI:

[10.1021/acs.jpca.7b11836](https://doi.org/10.1021/acs.jpca.7b11836)

Publication date:

2018

Document Version

Peer reviewed version

[Link to publication](#)

This document is the Accepted Manuscript version of a Published Work that appeared in final form in *Journal of Physical Chemistry A*, copyright © 2018 American Chemical Society after peer review and technical editing by the publisher. To access the final edited and published work see <http://doi.org/10.1021/acs.jpca.7b11836>.

University of Bath

Alternative formats

If you require this document in an alternative format, please contact:
openaccess@bath.ac.uk

General rights

Copyright and moral rights for the publications made accessible in the public portal are retained by the authors and/or other copyright owners and it is a condition of accessing publications that users recognise and abide by the legal requirements associated with these rights.

Take down policy

If you believe that this document breaches copyright please contact us providing details, and we will remove access to the work immediately and investigate your claim.

Computational Modelling of a Caged Methyl Cation: Structure, Energetics and Vibrational Analysis

Philippe B. Wilson^{a,b} and Ian H. Williams^{a*}

^a *Department of Chemistry, University of Bath, Claverton Down, Bath, BA2 7AY*

^b *Leicester School of Pharmacy, De Montfort University, The Gateway, Leicester, LE1 9BH*

Corresponding author

* Email: i.h.williams@bath.ac.uk

ORCID

Philippe B. Wilson: 0000-0003-0207-2246

Ian H. Williams: 0000-0001-9264-0221

ABSTRACT

DFT calculations for CH_3^+ within a constrained cage of water molecules permit the controlled manipulation of distances r_{ax} and r_{eq} to “axial” and “equatorial” waters. Equatorial $\text{CH}\cdots\text{O}$ interactions catalyze methyl transfer (MT) between axial waters. Variation in r_{ax} has a greater effect on CH bond lengths and stretching force constants in the symmetric $\text{S}_{\text{N}}2$ -like transition structures than variation in r_{eq} . In-plane bending frequencies are insensitive to these variations in cage dimensions, but axial interactions loosen the out-of-plane bending mode (OP) whereas equatorial interactions stiffen it. Frequencies for rotational and translational motions of CH_3^+ within the cage are influenced by r_{ax} and r_{eq} . In particular, translation of CH_3^+ in the axial direction is always coupled to cage motion. With longer r_{ax} , CH_3^+ translation is coupled with asymmetric CO bond stretching, but with shorter r_{ax} it is also coupled with OP (equivalent to the umbrella mode of trigonal bipyramidal $\text{O}\cdots\text{CH}_3^+\cdots\text{O}$); the magnitude of the imaginary MT frequency increases steeply as r_{ax} diminishes. This coupling between CH_3^+ and its cage is removed by eliminating the rows and columns associated with cage atoms from the full Hessian to obtain a reduced Hessian for CH_3^+ alone. Within a certain range of cage dimensions the reduced Hessian yields a real frequency for MT. The importance of using a Hessian large enough to describe the reaction-coordinate mode correctly is emphasised for modelling chemical reactions, and particularly for kinetic isotope effects in enzymic MT.

INTRODUCTION

Methyl transfer not only provides the prototypical example of an S_N2 mechanism but is also an important component of many biological processes, not least in reactions mediated by the *S*-adenosylmethionine (SAM) cofactor.¹ In view of methyl's small size, it is not obvious how an enzyme might preferentially stabilize the transition state (TS) for methyl transfer relative to the reactant state (RS). The observation of an inverse 2H_3 kinetic isotope effect (KIE) of unusually large magnitude, in the reaction of SAM with catecholate anion catalyzed by catechol O-methyltransferase (COMT), led to a hypothesis that catalysis might be facilitated by mechanical compression along the axis of the nucleophile and nucleofuge.² However, hybrid quantum-mechanical/molecular-mechanical (QM/MM) computational simulations of this KIE for methyl transfer in solution and in the active site of COMT did not support this hypothesis: the trend in the KIEs was reproduced but without any significant difference in the average distance between the methyl donor and acceptor atoms in the corresponding TSs.^{3,4} Nonetheless, an apparent trend in recent experimental 3H_3 KIEs for wild-type and mutant COMTs was interpreted as new evidence for compression.^{5,6} Meanwhile, a survey of high-resolution crystal structures⁷ has identified the functional importance of unconventional $CH\cdots O$ hydrogen bonding in SAM-dependent methyltransferases,⁷ and the essential role of an invariant tyrosine, which forms multiple $CH\cdots O$ hydrogen bonds to SAM in the active site of the lysine methyltransferase SET7/9, has been noted in an experimental study with mutated enzymes.⁸ $CH\cdots O$ hydrogen bonds have also been identified in QM/MM simulations for PRDM9 and Suv4-20h2 methyltransferases,^{9,10} and have been the subject of numerous QM studies (e.g. refs. 11 - 13 and many papers cited therein).

We recently reported QM calculations, for a model methyl-transfer reaction occurring inside a constrained cage of water molecules, that revealed a significant influence upon secondary (2°) $\alpha\text{-}^2H_3$ or $\alpha\text{-}^3H_3$ KIEs in response to controlled changes in $CH\cdots O$ interactions in the equatorial plane of the TS for a fixed donor-acceptor distance along the methyl-transfer axis.¹⁴ Whereas experimentally observed variations in 2° KIEs for enzyme-catalysed methyl transfer have been interpreted in terms of mediation of the distance between the methyl donor and acceptor groups in wild-type and mutant enzymes,^{5,6} our computational

results suggested that other factors might be responsible, at least in part.¹⁴ Here we describe (1) the influence of equatorial CH \cdots O interactions in catalysing S_N2-like methyl transfer along the axial direction within the same model cage, and (2) the influence of the whole cage upon the vibrational properties of the methyl cation (Me⁺) trapped within it. The model cage (Figure 1) permits the controlled manipulation of both the axial distance between donor/acceptor atoms and the equatorial distance to hydrogen-bond acceptors, thus providing a micro-reactor environment within which a range of structural and energetic variations on methyl transfer may be studied. We find that a defined range of cage sizes allow Me⁺ to exist as a discrete intermediate in S_N1-like methyl transfer, a mechanism that is not yet amenable to experimental observation. The separations between Me⁺ and axial O atoms considered in this study extend from the C \cdots O distance found in the unconstrained gas-phase S_N2 TS to longer range; the present purpose is not to re-investigate compression effects, either axially or in transverse directions.¹⁵

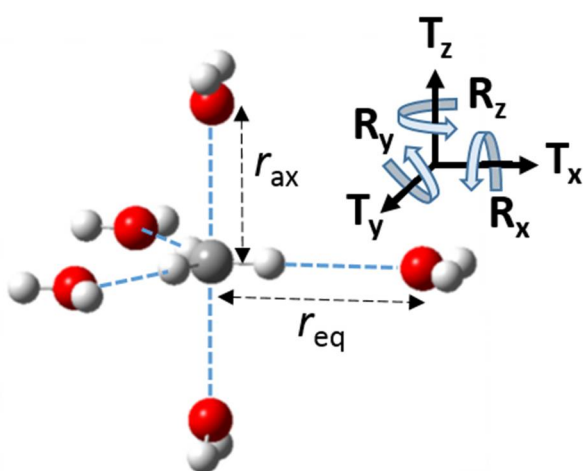


Figure 1. Geometry of the constrained cage complexed with methyl cation, together with axes defining methyl translations and rotations with respect to the cage.

METHODS

The cage comprises five water molecules arranged at the vertices of a trigonal bipyramid. Quasi- D_{3h} -symmetric structures are obtained by placing a methyl cation at its center, coplanar with the three equatorial waters and with collinear CH \cdots O_{eq} interactions, and perpendicular to the plane of the two axial waters. Each water molecule is frozen at particular fixed values of the C \cdots O_{ax} (r_{ax}) and C \cdots O_{eq} (r_{eq}) distances

in the symmetric structures and the rigid cage structure is maintained even when the methyl position is allowed to relax axially to form a tetrahedral CH_3OH_2^+ RS adduct with one of the axial waters.

Constrained geometry optimizations and analytical second-derivative calculations of Hessians were performed by means of the Gaussian09 program (revision A.02).¹⁶ The B3LYP density functional was used with the aug-cc-pVDZ basis set, a method previously identified as leading to reliable estimates of harmonic vibrational frequencies.¹⁷ Residual translational and rotational contributions to Hessian elements (punch=derivatives) were removed by a projection method^{18,19} in program CAMVIB, from our SULISO suite for vibrational analysis.²⁰ Atomic charges were evaluated using both electrostatic-potential (ESP) fitting and the atomic polar tensor (APT) method.

The whole system of cage and Me^+ has 57 degrees of freedom, including a number of small imaginary frequencies associated with displacements of water molecules away from their constrained positions and orientations. One way to isolate the Me^+ vibrational motions from those involving the cage H atoms is to eliminate all elements of the 57×57 Hessian in Cartesian coordinates except for the 12×12 block corresponding to Me^+ alone. Mass-weighting and diagonalization of this small block leads to 12 Me^+ frequencies: six internal (3 CH stretches, 2 in-plane bends, 1 out-of-plane bend) and six external (3 translations T_x , T_y and T_z and 3 rotations R_x , R_y and R_z , where z denotes the axial direction). The external modes have non-zero frequencies for rigid-body motion of Me^+ within its cage. In general the internal modes may be coupled to the external modes, but this coupling can be removed by means of projection of the Hessian into non-redundant internal coordinates defined by CH stretching, HCH bending and out-of-plane bending valence coordinates. This procedure yields zero frequencies for the six external modes, and six internal modes, which are uncoupled from the cage, but whose frequencies nonetheless still reflect the cage environment because the original Hessian is determined for the whole system. It is important to understand that the retained elements of the small Hessian are unchanged from their values in the large Hessian.

RESULTS AND DISCUSSION

Influence of Cage Dimensions on Interaction Energies and Methyl-Transfer Barriers. The potential energy of interaction between the constrained cage and Me^+ transferred from vacuum to the cage-center, in the TS geometry, becomes more negative as each of the distances r_{ax} and r_{eq} diminish (Figure 2a). Smaller cages provide more stabilization for the highly unstable methyl cation. Similar trends are found for the interaction energies in the RS geometry (see Supplementary Information for details) but the magnitudes are less pronounced. The B3LYP/aug-cc-pVDZ potential-energy barrier for the identity methyl transfer between unconstrained donor and acceptor water molecules within a gas-phase ion-molecule complex is 33.2 kJ mol^{-1} ; the overall OO distance ($2r_{\text{ax}}$) is 4.228 \AA in the RS and 3.968 \AA in the TS, very close to the axial dimension in the smallest constrained cage. The barrier height for methyl transfer within the constrained cage with $r_{\text{ax}} = 2.04 \text{ \AA}$ is lower than for the unconstrained reaction (even at $r_{\text{eq}} = \infty$) and becomes lower still as r_{eq} decreases. Strengthening of the equatorial $\text{CH}\cdots\text{O}$ interactions has a catalytic effect on methyl transfer. This catalysis is not the consequence of repulsive transverse compression by the equatorial waters within the confines of the constrained cage because the interaction of the cation with the cage is attractive and favors shorter r_{eq} distances. As r_{eq} decreases, the total charge on Me^+ becomes more positive, and the APT charge on each H atom increases, partially offset by a decrease of the C-atom charge. (See Supplementary Information for full details of energies and atomic charges.) For longer r_{ax} distances between the nucleophile and nucleofuge, the barriers to methyl transfer are higher than for the unconstrained reaction and increase with increasing r_{ax} , but are nonetheless dramatically reduced as r_{eq} decreases (Figure 2b). The increase in the barrier with increasing methyl-transfer distance may be rationalized simply in terms of the Principle of Least Nuclear Motion, as we have noted previously.²¹

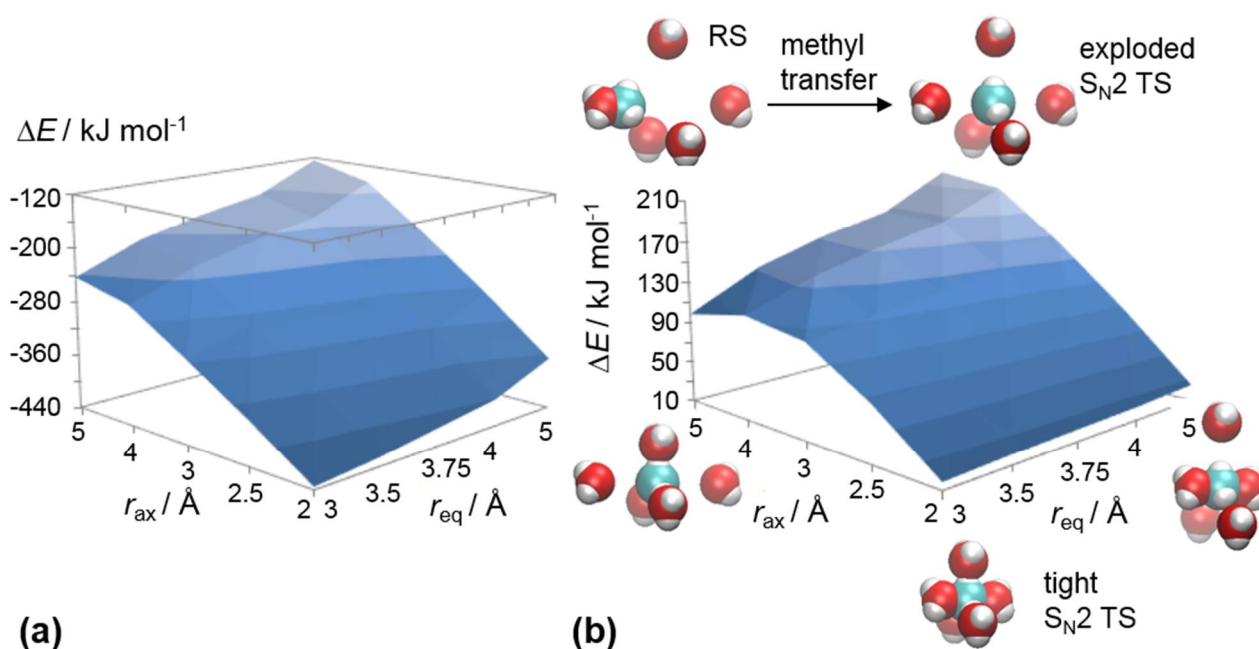


Figure 2. Variation in (a) interaction energy between methyl cation and the constrained water cage in the TS geometry and (b) potential energy barrier for methyl transfer from RS to TS within the cage as functions of cage dimensions r_{ax} and r_{eq} . All B3LYP/aug-cc-pVDZ energies in kJ mol^{-1} . Note that the distance axes are not to scale.

Influence of Cage Dimensions on Methyl CH Bond Lengths and Force Constants. Variation in r_{ax} has a greater effect on the average CH bond length (Figure 3a) and the average CH stretching force constant F (Figure 3b) than variation in r_{eq} and has a larger influence on the TS than the RS. (The precise values of $r_{\text{ax}} = 2.04$ and 2.525\AA are legacies from our earlier study²² on methyl cation in water treated within the polarised continuum model (PCM): the former is the PCM default radius for a carbon atom within the UFF cavity model, and the latter is the default radius for a CH_3 group within the UA0 cavity model.) As r_{ax} decreases, the TS bond length also decreases, but the force constant increases, suggesting a stiffening of the CH bonds in the transition structure with decreasing donor-acceptor distance. At $r_{\text{ax}} = \infty$, the optimum CH bond length in the planar energy-minimum geometry for $\text{Me}^+ \cdot 3\text{H}_2\text{O}$ is 1.1107\AA , with $r_{\text{eq}} = 2.9671 \text{\AA}$, very close to the TS values at $r_{\text{ax}} = 5.0 \text{\AA}$, $r_{\text{eq}} = 3.0 \text{\AA}$. As r_{eq} decreases, the TS bond length generally increases, and the force constant generally decreases, except for the shortest r_{ax} distances. This suggests that increasing the strength of equatorial $\text{CH} \cdots \text{O}$ interactions generally loosens the CH bonds in the TS. Figure 3 shows a maximum CH bond length (and minimum stretching force constant) in the TS for $r_{\text{ax}} = 2.04 \text{\AA}$ at $r_{\text{eq}} = 3.35 \text{\AA}$,

becoming shorter (and looser) at smaller values of r_{eq} ; this behavior is not explained by changes in the charge distribution, which all change gradually and monotonically with variations in r_{ax} and r_{eq} . Of course, the methyl group is trigonal-planar in each TS by symmetry, but in the RS it is tetrahedral, with average OCH angles that change smoothly over a small range as r_{ax} and r_{eq} are varied. (See Supplementary Information for more detail.)

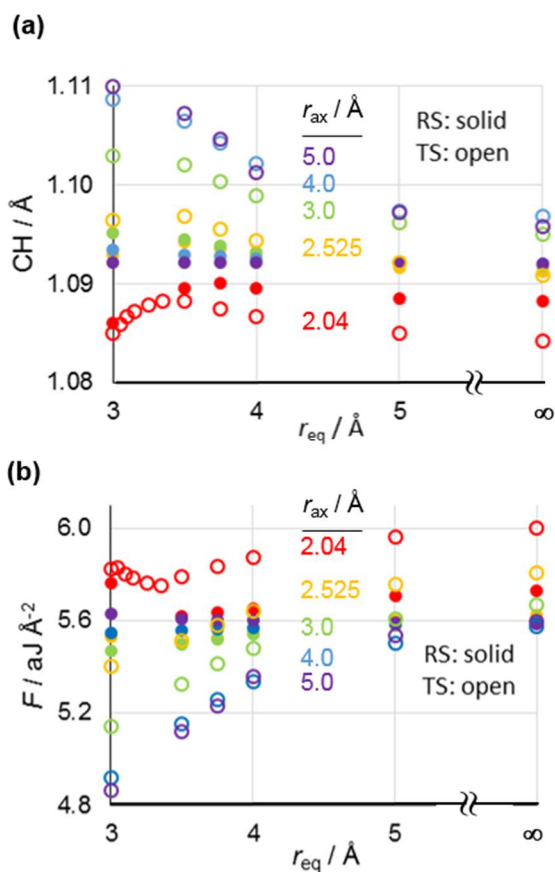


Figure 3. Variation in B3LYP/aug-cc-pVDZ (a) average CH bond length (\AA) and (b) average CH stretching force constant F (aJ \AA^{-2}) for the methyl group in the RS (solid circles) and TS (open circles) with distance r_{eq} within the constrained cage for $r_{\text{ax}} = 2.04$ (red), 2.525 (orange), 3.0 (green), 4.0 (blue) and 5.0 Å (purple).

Vibrational Analysis of the Caged Methyl Cation: Internal Modes. The average CH stretching frequency increases as the r_{ax} distance diminishes but decreases as the r_{eq} distance diminishes. Sandwiching Me^+ between the axial nucleophile/nucleofuge pair stiffens (and shortens) its CH bonds, whereas stabilizing interactions with equatorial H-bond acceptors loosen (and lengthen) them. These trends in vibrational frequencies are in accord with the results shown in Figure 3 for bond lengths and force constants. The lowest average frequency is 2969 cm^{-1} ($r_{\text{ax}} = 5 \text{ \AA}$, $r_{\text{eq}} = 3 \text{ \AA}$) and the highest is 3278 cm^{-1} ($r_{\text{ax}} = 2 \text{ \AA}$, $r_{\text{eq}} = 5 \text{ \AA}$);

these harmonic frequencies are certainly overestimated with respect to the best computational anharmonic prediction for gas-phase Me^+ (average 3052 cm^{-1} from vibrational configuration interaction with a coupled-cluster electronic structure method).²³ The average frequency (in the range $1390 - 1462\text{ cm}^{-1}$) for in-plane bending (IP) deformation is rather insensitive to r_{ax} but increases with diminishing r_{eq} as equatorial interactions strengthen. The out-of-plane bending (OP) frequency ($1274 - 1492\text{ cm}^{-1}$) decreases with diminishing r_{ax} but increases as r_{eq} diminishes: axial interactions loosen this mode but equatorial interactions stiffen it. These results for the six internal modes of Me^+ hold for frequencies obtained from both the full 57×57 and the reduced 12×12 Hessian; full details are provided in the Supplementary Information.

Vibrational Analysis of the Caged Methyl Cation: External Modes. The frequencies for the six external modes obtained from the reduced Hessian also respond to changes in the cage dimensions. The R_x and R_y modes are nearly degenerate, being split by the lack of true three-fold symmetry in the axial direction. The frequencies for both increase steeply as r_{ax} diminishes (from $320/320\text{ cm}^{-1}$ at $r_{\text{ax}} = 5\text{ \AA}$ to $1065/1032\text{ cm}^{-1}$ at $r_{\text{ax}} = 2\text{ \AA}$ and with $r_{\text{eq}} = 3\text{ \AA}$); they also rise gently as r_{eq} decreases. The same trend is found for both the full and reduced Hessians, although the frequencies obtained from the latter are slightly lower. The frequency of the R_z mode increases as r_{eq} diminishes (from 100 cm^{-1} at $r_{\text{eq}} = 5\text{ \AA}$ to 255 cm^{-1} at $r_{\text{eq}} = 3\text{ \AA}$ and with $r_{\text{ax}} = 5\text{ \AA}$), due to strengthening interactions with the equatorial waters of the cage, but it decreases as axial interactions become stronger with diminishing r_{ax} distance. However, as the equatorial $\text{CH}\cdots\text{O}$ interactions increase, so this mode becomes strongly coupled with in-plane rocking motions of the cage water molecules. This coupling is lost when the reduced Hessian is employed, and this leads to higher values for the R_z frequency at shorter r_{eq} distances.

A similar pattern emerges for the Me^+ translational modes. T_x and T_y are very nearly degenerate for all combinations of r_{ax} and r_{eq} except for the shortest axial dimension considered. Perhaps surprisingly, their frequencies are much more sensitive to r_{ax} than they are to r_{eq} , increasing from $26/26\text{ cm}^{-1}$ in a large cage ($r_{\text{ax}} = r_{\text{eq}} = 5\text{ \AA}$) to $148/131\text{ cm}^{-1}$ for T_x/T_y in the smallest cage ($r_{\text{ax}} = 2.04\text{ \AA}$, $r_{\text{eq}} = 3\text{ \AA}$). These modes also couple strongly with water-molecule deformations in smaller cages; for example, in the smallest cage a pair

of modes with frequencies of 326 and 285 cm^{-1} , respectively, involve rocking and scissoring of either axial or equatorial waters coupled with T_x or T_y .

In contrast to the other external modes of Me^+ within the cage, the full-Hessian frequency for methyl transfer between the axial waters is consistently imaginary for all cage sizes, corresponding to a reaction-coordinate mode, or transition vector, at a saddle point. It is important to note that in this mode Me^+ motion is always coupled to cage motion, primarily of the axial waters, but also of the equatorial waters for shorter values of r_{eq} . At larger values of r_{ax} , rigid translation T_z is coupled with the asymmetric combination (AS) of CO_{ax} bond stretching. However, for $r_{\text{ax}} < 3 \text{ \AA}$, T_z is also coupled with OP: in terms of the trigonal bipyramid formed by Me^+ and the axial O atoms, the methyl-transfer (MT) mode involves umbrella (UM) bending coupled to AS. The magnitude of the imaginary MT frequency increases steeply as r_{ax} diminishes (from $35i \text{ cm}^{-1}$ at $r_{\text{ax}} = 5 \text{ \AA}$ to $339i \text{ cm}^{-1}$ at $r_{\text{ax}} = 3 \text{ \AA}$ and with $r_{\text{eq}} = 3 \text{ \AA}$); for each value of r_{ax} the magnitude decreases gently as r_{eq} diminishes (solid circles in Figure 4). Vibrational coupling between Me^+ and the cage is removed by use of the reduced Hessian: the T_z frequency remains imaginary for all values of r_{eq} with $r_{\text{ax}} \leq 3 \text{ \AA}$, but with reduced magnitude (open circles in Figure 4). However, for $r_{\text{ax}} = 4$ or 5 \AA , there are ranges of r_{eq} within which the T_z frequency has a real value: specifically, for $r_{\text{ax}} = 4 \text{ \AA}$ T_z is real in the range $3.1 \leq r_{\text{eq}} \leq 3.5 \text{ \AA}$, and for $r_{\text{ax}} = 5 \text{ \AA}$ it is real for all values of r_{eq} . The maxima displayed in the plots of T_z frequency against r_{eq} for $r_{\text{ax}} = 4$ or 5 \AA are genuine and intriguing; they arise by removal of vibrational coupling between specific modes of the constrained cage and Me^+ , but we have no simple explanation for their appearance.

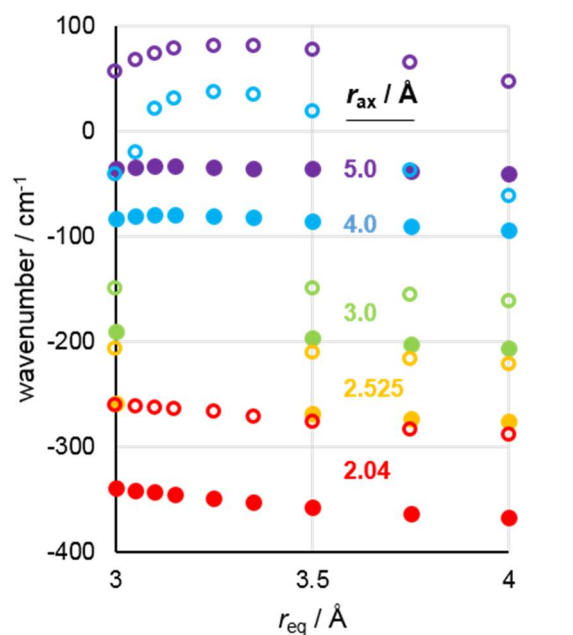


Figure 4. Variation of B3LYP/aug-cc-pVDZ unscaled harmonic frequencies (as wavenumbers / cm^{-1}) with distance r_{eq} for the methyl-transfer mode MT (solid circles, from the full Hessian) and the translational mode T_z (open circles, from the reduced Hessian) of methyl cation in the center of the constrained cage for $r_{\text{ax}} = 2.04$ (red), 2.525 (orange), 3.0 (green), 4.0 (blue) and 5.0 Å (purple). Negative values on the vertical axis correspond to imaginary frequencies.

Origin of the imaginary frequency for the methyl-transfer mode. It is instructive to enquire why the MT frequency for the full Hessian is always imaginary and why the T_z frequency is sometimes real. Consider first the smallest cage ($r_{\text{ax}} = 2.04$ Å, $r_{\text{eq}} = 3$ Å). The symmetry force constants for AS and UM both have positive values (0.06 aJ Å $^{-2}$ and 0.49 aJ rad $^{-2}$, respectively) and the off-diagonal coupling force constant is also positive (0.40 aJ Å $^{-1}$ rad $^{-1}$). The determinant of the 2×2 block of the full Hessian expressed in local symmetry coordinates is therefore given by $(0.06 \times 0.49) - (0.40)^2$, which is a negative value, meaning that one of the two eigenvalues must also be negative with an associated imaginary frequency. Similar analysis applies for other cage dimensions. Expressing the reduced Hessian in terms of the internal and external coordinates of Me^+ , the force constants for OP and T_z at $r_{\text{ax}} = 2.04$ Å, $r_{\text{eq}} = 3$ Å are 0.12 aJ rad $^{-2}$ and 0.02 aJ Å $^{-2}$, respectively, and the off-diagonal coupling force constant is (coincidentally) also 0.122 aJ Å $^{-1}$ rad $^{-1}$), making the 2×2 determinant equal to $(0.12 \times 0.02) - (0.12)^2$, which is obviously also a negative value, meaning that one of the two modes has an imaginary frequency. With some larger cages (for example, $r_{\text{ax}} = 4$ Å, $r_{\text{eq}} = 3.25$ Å), the force constants for OP and T_z are both positive but the coupling force constant is very

small, so that the corresponding determinant is $(0.41 \times 0.004) - (0.005)^2$, yielding a positive value consistent with both eigenvalues positive and both frequencies real. However, for most of the larger cages (for example, $r_{ax} = 3 \text{ \AA}$, $r_{eq} = 3 \text{ \AA}$), the force constant for T_z is negative and so also is the determinant, meaning that there is an imaginary frequency regardless of the sign or magnitude of the coupling force constant.

A discrete methyl cation intermediate within the cage? The fact that either the MT or the T_z frequency is imaginary for most combinations of r_{ax} and r_{eq} , implies that caged Me^+ is unstable with respect to translation perpendicular to its plane, and the system as a whole is an S_N2 -like TS. The absolute magnitude of the imaginary frequency increases for shorter r_{ax} distances, corresponding to tighter S_N2 TSs, but generally decreases a little as r_{eq} diminishes. The tighter the S_N2 TS is, the stronger the coupling is between T_z and OP, and the more the OP frequency and the magnitude of the T_z imaginary frequency are raised. However, the coupling can be removed by projecting out the external modes: this “raises” the imaginary T_z frequency to zero and lowers the OP frequency, by $>600 \text{ cm}^{-1}$ at the shortest r_{ax} distances, with what is now a 6×6 Hessian expressed in internal coordinates only. The very weak coupling between OP with T_z at long r_{ax} distances that leads to some real T_z frequencies within certain ranges of r_{eq} might appear to imply that Me^+ is stable with respect to translation in the axial direction for methyl transfer in these cages: in other words, that it is an intermediate for S_N1 -like methyl transfer. However, it should be recalled that the MT frequency arising from the full Hessian is still always imaginary. Although it is computationally possible, as above, to analyse the vibrational structure of Me^+ as a discrete entity using Hessian elements obtained for the full system but with removal of its coupling with the cage, it is not physically possible to disengage Me^+ from its environment. Nonetheless, it is of interest to note that the $2^\circ \text{ } ^2\text{H}$ KIE for methyl transfer between the axial water molecules (the nucleophile and nucleofuge) within the cage at $r_{ax} = 4 \text{ \AA}$, $r_{eq} = 3.25 \text{ \AA}$ is calculated to be about 1.43 per deuterium at 298 K, as compared with about 1.06 per deuterium at $r_{ax} = 2 \text{ \AA}$, $r_{eq} = 3 \text{ \AA}$. The latter involves a tight S_N2 -like TS whereas the former involves a very loose (exploded) S_N2 -like TS with a high degree of S_N1 character. Of course, S_N1 methyl transfer is not observed experimentally, since this mechanism is strongly disfavoured under normal reaction conditions. It is intriguing to speculate

whether there might exist a stable nanoporous material, or an organic host, with appropriate cavity dimensions such that within it a methyl cation might be a discrete intermediate.

Bickelhaupt and co-workers have described how the C atom in an S_N2 TS $[\text{Cl}\cdots\text{CH}_3\cdots\text{Cl}]^-$ is too small to fill the trigonal bipyramidal cage of the axial Cl^- and equatorial H atoms and therefore prefers a position closer to one of the Cl atoms in an RS of lower energy.²⁴ As we had also done earlier,²¹ he has noted that D_{3h} -symmetrical noble-gas complexes $[\text{Ng}\cdots\text{CH}_3\cdots\text{Ng}]^+$ are energy-minimum structures for $\text{Ng} = \text{He}$ or Ne but are S_N2 TSs for $\text{Ng} = \text{Ar}$ or Kr .²⁵ However, Me^+ sandwiched between two helium or neon atoms is not an intermediate for S_N1 methyl transfer between them, and the helium or neon dimer does not provide a stable cavity within which to host Me^+ as a guest.

Requirements for an adequate methyl-transfer reaction coordinate. In the past, computational studies of reactions in solution or in an enzyme active site have often employed a “cut-off” strategy to truncate the size of the system in order to render a tractable model in regard to limitations of available computational resources: groups of atoms beyond a certain distance from the reaction center are assumed to have negligible effect upon the reactive behaviour and therefore are removed from the model. For example, a continuum model of solvation may be employed, in which solvent molecules are not treated explicitly, and this may allow for an adequate description of the particular properties of the system under consideration. On the other hand, where specific solvent interactions are important, this type of description may not be adequate. It is never realistic to treat the protein environment of an enzyme-catalyzed reaction as a homogeneous continuum, but nonetheless calculations of isotope effects for these reactions commonly use cut-off models.²⁶ The present study shows how structures, energetics and vibrational properties may be affected by interactions between the CH bonds of a transferring methyl group and hydrogen-bond acceptors in their proximity. Our previous study of 2° $\alpha\text{-}^2\text{H}_3$ and $\alpha\text{-}^3\text{H}_3$ KIEs for methyl transfer within the same constrained cage concluded that these effects may be modulated by $\text{CH}\cdots\text{O}$ hydrogen bonding interactions with groups in the equatorial region of the TS.¹⁴ A recent computational study of the reaction catalysed by glycine *N*-methyltransferase also indicates the importance of hydrogen-bonding interactions between active-site residues of the CH bonds of the transferring methyl.²⁷ These results all shed additional

light which may help to resolve a current controversy regarding the catalytic mechanisms of enzymic methyl-transfer reactions.^{3-6,28,29} In order to ensure that isotope effects, upon both substrate binding and reaction kinetics, are adequately described in computational models, it is essential that groups possibly involved in hydrogen-bonding interactions with the transferring methyl group are incorporated in Hessians computed for these systems. The key point to be made in the light of the present study is that the inclusion or exclusion of certain atoms or groups may have a significant influence, both quantitatively and qualitatively, on the nature of the all-important reaction-coordinate mode in the TS that determines both mechanism and KIEs. Although this study has considered KIEs only in passing (since the influence of “cut-off” procedures on the description of the reaction coordinate, and the implications for KIEs, will be the explicit focus of a subsequent paper), it is worth emphasising here that CH \cdots O hydrogen-bonding interactions with Me⁺ make normal contributions to 2° α -²H₃ and α -³H₃ KIEs for methyl transfer, as demonstrated in our previous work¹⁴ and contrary to an assertion that they contribute inversely.³⁰ It has long been known that CH stretching vibrations always make inverse contributions,³¹ and that the overall direction of a 2° α -KIE is determined by the other (mostly bending) modes whose contribution may be either inverse or normal.²¹

CONCLUSIONS

Controlled manipulation of the axial donor/acceptor distance and the equatorial distance to hydrogen-bond acceptors for methyl cation complexed within a constrained cage of water molecules reveals that CH \cdots O interactions with equatorial waters exert a catalytic effect on methyl transfer between axial waters. Variation in r_{ax} has a greater effect on CH bond lengths and stretching force constants in the symmetric S_N2-like TSs than variation of the equatorial distance. IP frequencies are insensitive to these variations in cage dimensions, but axial interactions loosen the OP mode whereas equatorial interactions stiffen it. Frequencies for rotational and translational motions of Me⁺ within the cage are influenced by the axial and equatorial distances. In particular, T_z is always coupled to cage motion. With longer r_{ax} , T_z is coupled with the asymmetric combination of CO bond stretching, but with shorter r_{ax} it is also coupled with OP

(equivalent to the umbrella mode of the $[O\cdots Me^+\cdots O]$ trigonal bipyramid); the magnitude of the imaginary methyl-transfer frequency increases steeply as the axial nucleophile-nucleofuge distance diminishes. This coupling between Me^+ and its cage may be removed by eliminating the rows and columns associated with cage atoms from the full Hessian to obtain a reduced Hessian for Me^+ alone. Within a certain range of cage dimensions the reduced Hessian yields a real frequency for the methyl-transfer mode. The importance of using a Hessian large enough to describe the reaction-coordinate mode correctly is emphasised for modelling chemical reactions, and particularly for KIEs in enzymic methyl transfer.

ASSOCIATED CONTENT

Supporting Information

Geometries, energies, selected force constants and vibrational frequencies for optimized structures, and complete ref 15. This material is available free of charge via the Internet at <http://pubs.acs.org>.

AUTHOR INFORMATION

Corresponding Author

E-mail i.h.williams@bath.ac.uk. Phone: +44 1225 386625. Fax +44 1225 386231.

Notes

The authors declare no competing financial interest.

ACKNOWLEDGMENTS

EPSRC is thanked for a DTA Studentship (PBW). This research made use of the Balena High Performance Computing (HPC) Service at the University of Bath.

REFERENCES

- (1) Struck, A.-W.; Thompson, M. L.; Wong, L. S.; Micklefield, J. S-Adenosyl-Methionine-Dependent Methyltransferases: Highly Versatile Enzymes in Biocatalysis, Biosynthesis and other Biotechnological Applications. *ChemBioChem* **2012**, *13*, 2642–2655.
- (2) Hegazi, M. F.; Borchardt, R. T.; Schowen, R. L. α -Deuterium and Carbon-13 Isotope Effects for Methyl Transfer Catalyzed by Catechol O-Methyltransferase. S_N2 -Like Transition-State. *J. Am. Chem. Soc.* **1979**, *101*, 4359-4365.
- (3) Ruggiero, G. D.; Williams, I. H.; Roca, M.; Moliner, V.; Tuñón, I. QM/MM Determination of Kinetic Isotope Effects for COMT-Catalyzed Methyl Transfer Does Not Support Compression Hypothesis. *J. Am. Chem. Soc.* **2004**, *126*, 8634–8635.
- (4) Kanaan, N.; Ruiz-Pernía, J. J.; Williams, I. H. QM/MM Simulations for Methyl Transfer in Solution and Catalysed by COMT: Ensemble-Averaging of Kinetic Isotope Effects. *Chem. Commun.* **2008**, 6114-6116.
- (5) Zhang, J. Y.; Klinman, J. P. Enzymatic Methyl Transfer: Role of an Active Site Residue in Generating Active Site Compaction That Correlates with Catalytic Efficiency. *J. Am. Chem. Soc.* **2011**, *133*, 17134–17137.
- (6) Zhang, J. Y.; Kulik, H. J.; Martinez, T. J.; Klinman, J. P. Mediation of Donor-Acceptor Distance in an Enzymatic Methyl Transfer Reaction. *Proc. Natl. Acad. Sci. U. S. A.* **2015**, *112*, 7954–7959.
- (7) Horowitz, S.; Dirk, L. M. A.; Yesselman, J. D.; Nimtz, J. S.; Adhikari, U.; Mehl, R. A.; Scheiner, S.; Houtz, R. L.; Al-Hashimi, H. M.; Trievel, R. C. Conservation and Functional Importance of Carbon–Oxygen Hydrogen Bonding in AdoMet-Dependent Methyltransferases. *J. Am. Chem. Soc.* **2013**, *135*, 15536–15548.
- (8) Horowitz, S.; Adhikari, U.; Dirk, L. M. A.; Del Rizzo, P. A.; Mehl, R. A.; Houtz, R. L.; Al-Hashimi, H. M.; Scheiner, S.; Trievel, R. C. Manipulating Unconventional CH-Based Hydrogen Bonding in a Methyltransferase via Noncanonical Amino Acid Mutagenesis. *ACS Chem. Biol.* **2014**, *9*, 1692-1697.
- (9) Chu, Y.; Sun, L.; Zhong, S. How Y357F, Y276F Mutants Affect the Methylation Activity of PRDM9: QM/MM MD and Free Energy Simulations. *J. Mol. Model.* **2015**, *21*, art. 125.
- (10) Qian, P.; Guo, H.; Wang, L.; Guo, H. QM/MM Investigation of Substrate and Product Specificities of Suv4-20h2: How Does This Enzyme Generate Dimethylated H4K20 from Monomethylated Substrate? *J. Chem. Theory Comput.* **2017**, *13*, 2977–2986.
- (11) Scheiner, S. Theoretical Analysis of the Contributions Made by CH \cdots OH Bonds to Protein Structure. *Curr. Org. Chem.* **2010**, *14*, 106-128.
- (12) Scheiner, S. Dissection of the Factors Affecting Formation of a CH \cdots O H-Bond. A Case Study. *Crystals* **2015**, *5*, 327-345.
- (13) Moore, K. B.; Sadeghian, K.; Sherrill, C. D.; Ochsenfeld, C.; Schaefer, H. F. C–H \cdots O Hydrogen Bonding. The Prototypical Methane-Formaldehyde System: A Critical Assessment. *J. Chem. Theory Comput.* **2017**, *13*, 5379–5395.
- (14) Wilson, P. B.; Williams, I. H. Influence of Equatorial CH \cdots O Interactions on Secondary Kinetic Isotope Effects for Methyl Transfer. *Angew. Chemie Int. Ed.* **2016**, *55*, 3192–3195.
- (15) Wolfe, S.; Kim, C.-K.; Yang, K.; Weinberg, N.; Shi, Z. Transverse Compression and the Secondary H/D Isotope Effects in Intramolecular S_N2 Methyl-Transfer Reactions. *Can. J. Chem.* **1998**, *76*, 359-370.
- (16) Frisch, M. J.; Trucks, G. W.; Schlegel, H. B.; Scuseria, G. E.; Robb, M. A.; Cheeseman, J. R.; Scalmani, G.; Barone, V.; Mennucci, B.; Petersson, G. A., et al. *Gaussian 09*, revision A.02. Gaussian, Inc.: Wallingford, CT, USA 2009.
- (17) Wilson, P. B.; Williams, I. H. Critical Evaluation of Anharmonic Corrections to the Equilibrium Isotope Effect for Methyl Cation Transfer from Vacuum to Dielectric Continuum. *Mol. Phys.* **2015**, *113*, 1704–1711.

- (18) Williams, I. H. On the Representation of Force Fields for Chemically Reacting Systems. *Chem. Phys. Lett.* **1982**, *88*, 462-466.
- (19) Williams, I. H. Force-Constant Computations in Cartesian Coordinates. Elimination of Translational and Rotational Contributions. *J. Mol. Struct. THEOCHEM* **1983**, *11*, 275-284.
- (20) Williams, I. H.; Wilson, P. B. SULISO: The Bath Suite of Vibrational Characterization and Isotope Effect Calculation Software. *SoftwareX* **2017**, *6*, 1-6.
- (21) Ruggiero, G. D.; Williams, I. H. Kinetic Isotope Effects for Gas Phase S_N2 Methyl Transfer: a Computational Study of Anionic and Cationic Identity Reactions. *J. Chem. Soc., Perkin Trans. 2* **2002**, 591-597.
- (22) Wilson, P. B.; Weaver, P. J.; Greig, I. R.; Williams, I. H. Solvent Effects on Isotope Effects: Methyl Cation as a Model System. *J. Phys. Chem. B* **2015**, *119*, 802-809.
- (23) Cunha de Miranda, B. K.; Alcaraz, C.; Elhanine, M.; Noller, B.; Hemberger, P.; Fisher, I.; Garcia, G. A.; Soldi-Lose, H.; Bérenger, G.; Vieira Mendes, L. A.; Boyé-Péronne, S.; Douin, S.; Zabka J.; Botschwina, P. Threshold Photoelectron Spectroscopy of the Methyl Radical Isotopomers, CH₃, CH₂D, CHD₂ and CD₃: Synergy Between VUV Synchrotron Radiation Experiments and Explicitly Correlated Coupled Cluster Calculations. *J. Phys. Chem. A* **2010**, *114*, 4818-4830.
- (24) Pierrefixe, S. C. A. H.; Fonseca Guerra, C.; Bickelhaupt, F. M. Hypervalent Silicon versus Carbon: Ball-in-a-Box Model. *Chem. Eur. J.* **2008**, *14*, 819 – 828.
- (25) Pierrefixe, S. C. A. H.; Poater, J.; Im, C.; Bickelhaupt, F. M. Hypervalent versus Nonhypervalent Carbon in Noble-Gas Complexes. *Chem. Eur. J.* **2008**, *14*, 6901-6911.
- (26) Williams, I. H.; Wilson, P. B. In *Simulating Enzyme Reactivity*; Tuñón, I., Moliner, V., Eds.; Royal Society of Chemistry: Cambridge, U. K., 2017
- (27) Świderek, K.; Tuñón, I.; Williams, I. H.; Moliner, V. DAD's Not in Charge of Me: Insight on Glycine N-Methyltransferase Catalysis from Computational Modelling. *Submitted for publication*.
- (28) Zhang, J.; Klinman, J. P. Convergent Mechanistic Features between the Structurally Diverse N- and O-Methyltransferases: Glycine N-methyltransferase and Catechol O-methyltransferase. *J. Am. Chem. Soc.* **2016**, *138*, 9158-9165.
- (29) Lameira, J.; Bora, R. P.; Chu, Z. T.; Warshel, A. Methyltransferases Do Not Work by Compression, Cratic, or Desolvation Effects, But by Electrostatic Preorganization. *Proteins: Struct. Funct. Genet.* **2015**, *83*, 318-330.
- (30) Linscott, J. A.; Kapilashrami, K.; Wang, Z.; Senevirathne, C.; Bothwell, I. R.; Blum, G.; Luo, M. Kinetic Isotope Effects Reveal Early Transition State of Protein Lysine Methyltransferase SET8. *Proc. Natl. Acad. Sci. U. S. A.* **2016**, *113*, E8369-E8378.
- (31) Williams, I.H. Theoretical Modelling of Compression Effects in Enzymic Methyl Transfer. *J. Am. Chem. Soc.* **1984**, *106*, 7206-7212.

Table of Contents Graphic

